

Do Lognormal Column-Density Distributions in Molecular Clouds Imply Supersonic Turbulence?

K. Tassis¹, D. A. Christie², A. Urban¹, J. L. Pineda¹, T. Ch. Mouschovias², H. W. Yorke¹, H. Martel^{3,4}

¹*Jet Propulsion Laboratory, California Institute of Technology, Pasadena, CA 91109, USA*

²*Departments of Physics and Astronomy, University of Illinois at Urbana-Champaign, 1002 W. Green Street, Urbana, IL 61801, USA*

³*Département de Physique, de Génie Physique et d'Optique, Université Laval, Québec, QC, G1K7P4, Canada*

⁴*Centre de Recherche en Astrophysique du Québec*

11 June 2018

ABSTRACT

Recent observations of column densities in molecular clouds find lognormal distributions with power-law high-density tails. These results are often interpreted as indications that supersonic turbulence dominates the dynamics of the observed clouds. We calculate and present the column-density distributions of three clouds, modeled with very different techniques, none of which is dominated by supersonic turbulence. The first star-forming cloud is simulated using smoothed particle hydrodynamics (SPH); in this case gravity, opposed only by thermal-pressure forces, drives the evolution. The second cloud is magnetically subcritical with subsonic turbulence, simulated using nonideal MHD; in this case the evolution is due to gravitationally-driven ambipolar diffusion. The third cloud is isothermal, self-gravitating, and has a smooth density distribution analytically approximated with a uniform inner region and an r^{-2} profile at larger radii. We show that in all three cases the column-density distributions are lognormal. Power-law tails develop only at late times (or, in the case of the smooth analytic profile, for strongly centrally concentrated configurations), when gravity dominates all opposing forces. It therefore follows that lognormal column-density distributions are generic features of diverse model clouds, and should not be interpreted as being a consequence of supersonic turbulence.

Key words: ISM: clouds — ISM: structure — stars: formation — methods: numerical — methods: statistical — turbulence

1 INTRODUCTION

Recent observations indicate that the column-density distribution in molecular clouds is typically lognormal. For example, Goodman et al. (2009) studied the Perseus molecular cloud using 2MASS, IRAS, and ^{13}CO data, and found that the column-density distributions of both the cloud as a whole and that of smaller, few-parsec “subregions” are lognormal. Kainulainen et al. (2009) probed the column-density distributions in 23 molecular cloud complexes using near-infrared dust extinction maps from the 2MASS data archive, also finding lognormal column density distributions, with power-law tails present in star forming clouds. Lombardi, Alves, & Lada (2006) analyzed 2MASS data for the Pipe nebula and found that the column-density distributions are complex; however because multiple velocity components are present in C^{18}O (Onishi et al. 1999; Muench et al. 2007), the complexity may be the effect of superposition of more than

one cloud observed in projection, and the underlying individual components may still be consistent with lognormal distributions. Wong et al. (2008) observed the column-density distribution of the Giant Molecular Cloud RCW 106 in ^{13}CO and found it to be lognormal. Finally, Pineda et al. (2010) also found lognormal column-density distributions with tails for the Taurus molecular cloud using 2MASS extinction and CO observations.

These results have been attributed to the dominance of supersonic turbulence in the observed regions. When gas turbulent pressure dwarfs the thermal-pressure term with negligible gravitational and magnetic forces, the hydrodynamic equations become scale invariant, and the distribution of the volume density accordingly becomes lognormal (Vázquez-Semadeni 1994). Ostriker et al. (2001) have shown that, in highly supersonic turbulent ideal-MHD simulations including self-gravity, the column-density distribution is also lognormal. Vázquez-Semadeni & García (2001) examined tur-

arXiv:1006.2826v1 [astro-ph.GA] 14 Jun 2010

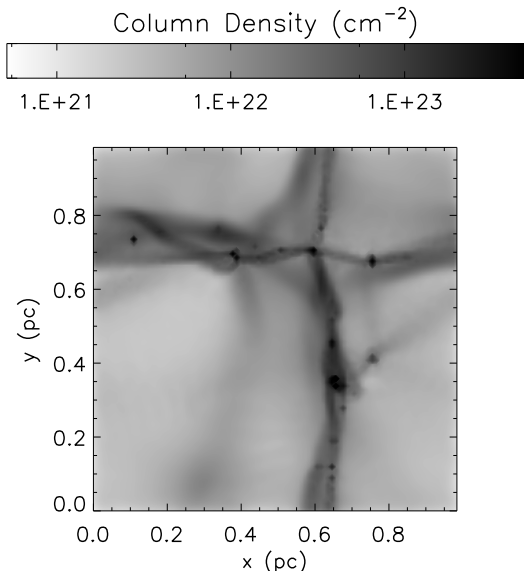


Figure 1. Column-density map of simulation A at $t = 0.72$ Myr. The grayscale corresponds to the (logarithmic) column-density scale.

bulent 3-dimensional simulations, both magnetic and non-magnetic, as well as random realizations of 3-dimensional lognormal density fields. They argued that the shape of the column-density distribution depends on the number of correlation lengths included in the line-of-sight over which the density integration occurs. As the integration path increases from less than one to many correlation lengths, the column-density distribution transitions from lognormal (the underlying 3-dimensional density field distribution) to exponential, to Gaussian (due to the central limit theorem, when many uncorrelated patches are summed up along the line of sight). They proposed to invert the argument to derive from the observed shape of the column-density distribution the number of correlation lengths in clouds along the line of sight. They suggested that the reason for which column density distributions are found to be lognormal with exponential tails in simulations is that too few correlation lengths are included to render the distributions Gaussian. Federrath et al. (2009) find, in purely hydrodynamic isothermal simulations with supersonic turbulence and no self-gravity, lognormal volume- and column-density distributions, the width of which depends on the driving mechanism – since these are driven turbulence simulations. Small deviations in the wings, mostly in the low-density wing, were attributed to intermittency of the velocity field.

Although these studies establish that model molecular clouds dominated by supersonic turbulence exhibit lognormal distributions of column densities, they do not demonstrate that the dominance of supersonic turbulence is the prime cause of such column-density distributions or even that supersonic turbulence is a necessary ingredient. In other words, there may be other features of the assumed model clouds that are responsible for this effect. *Even if* dominance of supersonic turbulence is a *sufficient* condition to produce lognormal column-density distributions, it does not follow that it is also a *necessary* condition.

In this paper we test the uniqueness of the supersonic-

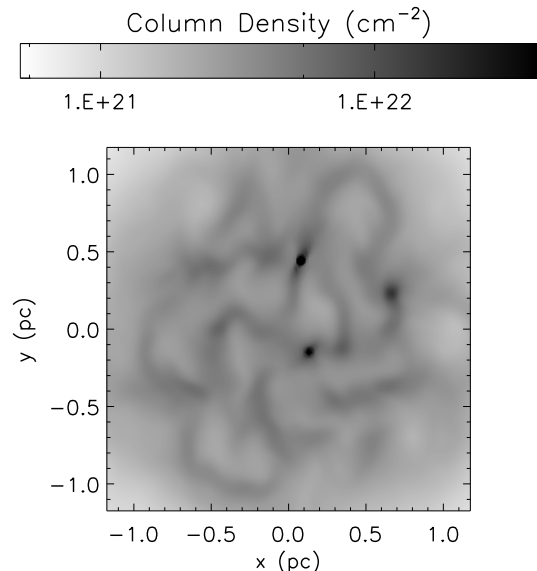


Figure 2. Column-density map of simulation B at $t = 4.8$ Myr. The grayscale corresponds to the (logarithmic) column-density scale.

turbulence interpretation and study the ubiquity of lognormal column-density distributions. In particular, we investigate whether lognormal column-density distributions can also be produced in model molecular clouds *not* dominated by supersonic turbulence. We do so by examining the column-density distributions in three very different examples of model molecular clouds. In the first example, the molecular cloud is simulated using Smoothed Particle Hydrodynamics (SPH, Monaghan 1992), including self-gravity and radiative heating/cooling. In the second example, a 3-dimensional, magnetically subcritical molecular cloud evolves due to gravitationally-driven ambipolar diffusion in the presence of *subsonic* turbulence. In the third example, we examine the analytically approximated density distribution of an isothermal, self-gravitating cloud having a uniform-density central region and a power-law profile at larger radii (Dapp & Basu 2009).

In §2 we present the basic relevant properties of the three model clouds and discuss the evolution of the first two – the third one is a static model. In §3 we present and discuss the column-density distributions in each of the model clouds, and their dependence on time or on profile parameters as appropriate. The conclusions are summarized in §4.

2 THE MODEL CLOUDS

The first simulation (simulation A) is described in detail in Urban et al. (2010a, 2010b). Here we briefly summarize its main features. It uses the SPH algorithm with particle splitting and sink particles (Martel et al. 2006). The simulation box is approximately 1 pc^3 in volume with periodic boundary conditions. It contains a total mass of $670 M_{\odot}$. The material is initially distributed uniformly with small density perturbations that reproduce a Gaussian random field with a density power spectrum $P(k) \propto k^{-2}$. The initial density of the region is $n = 1.22 \times 10^4 \text{ cm}^{-3}$ and the initial

temperature is $T = 5$ K. Sink particles (which can be interpreted as single stars or groups of stars) form at a density $n = 7.3 \times 10^7 \text{ cm}^{-3}$ or mass $0.008 M_\odot$. The simulation is stopped when the highest sink-particle mass reaches $21 M_\odot$. In addition to gravity, the simulation also includes heating and cooling of both gas and dust. The radiative effect of forming stars is included using the algorithm described in Urban et al. (2009). The luminosity from the young stars (sink particles) heats the dust, which is collisionally coupled to the gas. Molecular cooling and heating from cosmic-ray ionisation is also included in the calculation of the gas temperature. A column-density map of simulation A at $t = 0.72$ Myr, which is the final time, is shown in Fig. 1.

The second simulation (simulation B) is an MHD run using Zeus-MP (Hayes et al. 2006) which has been extended to include ambipolar diffusion. The simulation box is $8 \text{ pc} \times 8 \text{ pc} \times 2 \text{ pc}$ with the third dimension being the direction of the initial $16.3 \mu\text{G}$ magnetic field. The MHD boundary conditions are reflective and the boundary conditions on the gravitational field are appropriate for an isolated cloud. The initial density distribution is $n = 300 \text{ cm}^{-3}$ within a cylindrical radius of 2 pc , and with a Gaussian tail beyond that¹. The initial central mass-to-(magnetic)flux ratio is 0.9 times the critical value for collapse. The cloud is allowed to relax to equilibrium before a Gaussian random velocity field (with subsonic root-mean-square velocity dispersion $\simeq 0.5 C_s$ (where C_s is the isothermal sound speed) is introduced and ambipolar diffusion is turned on. The simulation is stopped when the maximum density reaches $5 \times 10^6 \text{ cm}^{-3}$. The column-density map at this time ($t = 4.8$ Myr), looking down the initial direction of the magnetic field, is shown in Fig. 2. At this time, there are eighteen identifiable self-gravitating cores, separated by a mean distance $\simeq 0.3 \text{ pc}$, and with a range of masses $0.32 - 15 M_\odot$. More details for this run and other, similar runs, but with different input parameters, are given in Christie & Mouschovias (2010).

The third case we examine is an approximate, analytic, *smooth* density profile, without any random perturbations. The analytic expression is designed to fit a spherical, isothermal cloud, with a flat inner region and a power-law density profile at larger radii (a Bonnor-Ebert sphere, with only thermal pressure opposing gravity, and not necessarily in equilibrium):

$$\rho(r) = \begin{cases} \rho_c a^2 / (r^2 + a^2) & r \leq R \\ 0 & r > R \end{cases}, \quad (1)$$

where ρ_c is the central value of the density, R is the radius of the cloud, and the parameter a determines the size of the uniform-density inner region and is proportional to the Jeans length. The column density for this cloud is then (Dapp &

¹ This low-density “envelope”, beyond the inner 2 pc region of the model cloud, is added for computational convenience (to avoid reflection of waves). It does not have any physical significance, so it is not shown in the display of the physical results. The results are not affected by its presence, provided that its size is large enough.

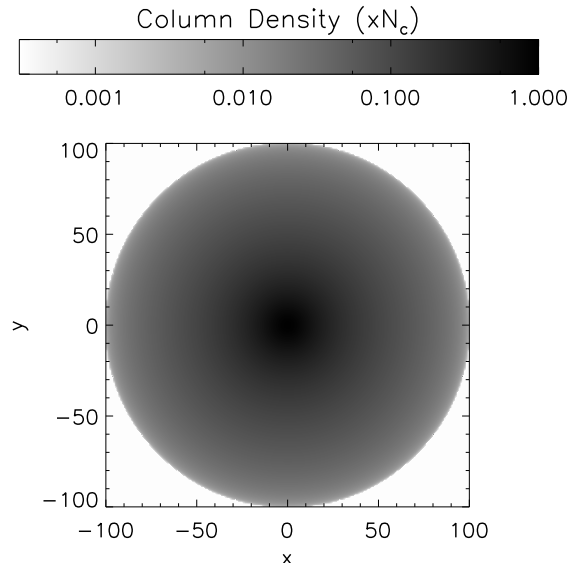


Figure 3. Column density of a cloud with a smooth density profile given by Eq. (1) and $(a, c) = (10, 10)$.

Basu 2009)

$$N(\tilde{r}) = \frac{N_c}{\sqrt{1 + (\tilde{r}/a)^2}} \times \left[\arctan \left(\sqrt{\frac{c^2 - (\tilde{r}/a)^2}{1 + (\tilde{r}/a)^2}} \right) / \arctan(c) \right], \quad (2)$$

where N_c is the central value of the column density, \tilde{r} is the radial coordinate on the plane of the sky, and $c = R/a$, the size of the cloud relative to that of the uniform-density central region. We sample this profile with a 1024×1024 grid, and we then construct a distribution of the column-density values within the grid. We examine two cases of this profile. The first has $(a, c) = (10, 10)$ and corresponds to a cloud with a substantial flat inner region compared to the total volume of the cloud. The central gas density is 101 times greater than the density at the surface of the cloud. A column-density map of this cloud is shown in Fig. 3. The second case has $(a, c) = (2, 350)$ and represents a much more centrally concentrated cloud (in the limit $a \rightarrow 0, c \rightarrow \infty$ the profile becomes a singular isothermal sphere). For the second case the central gas density is $\sim 10^5$ times greater than the density at the surface of the cloud.

3 RESULTS

The results for simulations A and B are summarized in Figs. 4 and 5 in which we show snapshots at different times of the column-density distribution (represented in the form of a histogram) in each simulation. The time corresponding to each snapshot is indicated as a label in each panel. The lower horizontal axis shows the column density in units of cm^{-2} while the upper axis shows extinction (A_V) using the conversion $N_{\text{H}_2}/A_V = 9.4 \times 10^{20} \text{ cm}^{-2}/\text{mag}$ (Bohlin et al. 1978). For simulation A, the column density is sampled with a 100×100 grid, using 51 logarithmically-spaced bins, spanning column density values from 1.5×10^{20} to $2 \times 10^{23} \text{ cm}^{-2}$.

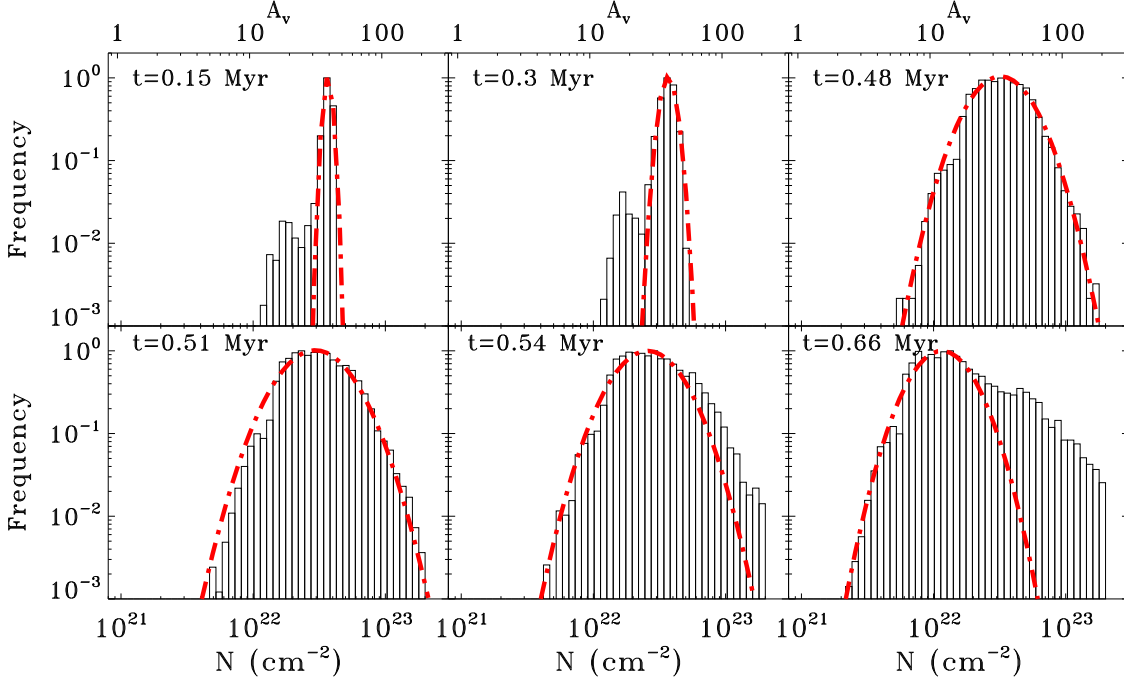


Figure 4. Snapshots at different times of the column-density distribution in a molecular cloud, whose evolution is followed using an SPH code (simulation A). The evolution is initiated and controlled by self-gravity, and proceeds at the free-fall timescale. The dot-dashed line is the best fit lognormal that describes the histograms. The high column-density tail develops at late times due to the formation of cores and protostars inside the molecular cloud.

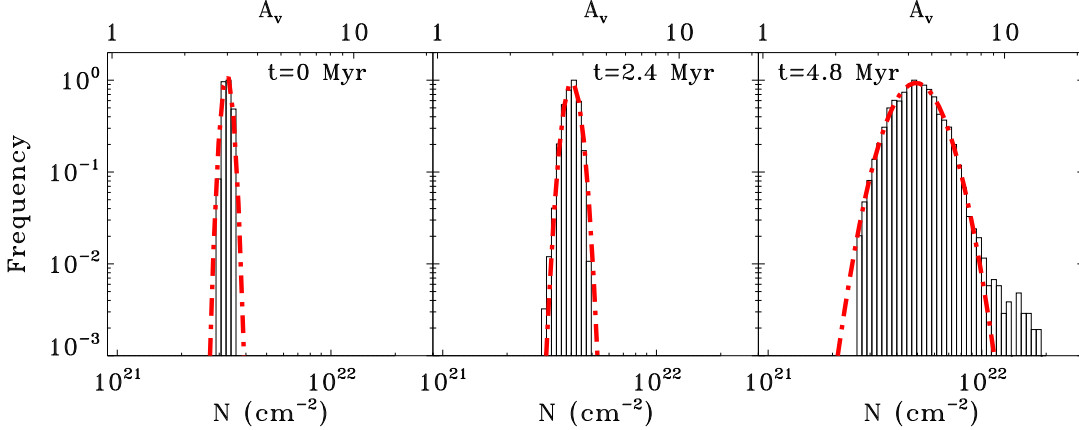


Figure 5. Snapshots at different times of the column-density distribution in a molecular cloud, whose evolution is followed using a 3D, nonideal MHD code (simulation B). The evolution observed here is due to gravitationally-driven ambipolar diffusion. The dot-dashed line is the best fit lognormal that describes the histograms.

For simulation B, the distribution of column densities in the central 2.3×2.3 pc is sampled using again 51 logarithmically spaced bins, now spanning column density values from 8×10^{20} to 2×10^{22} cm^{-2} . In this region, the simulation grid is uniform and it has 118×118 cells. The velocity dispersions increase in each snapshot with increasing time, from $0.48C_s$ at $t = 0$ to $0.55C_s$ at $t = 2.4$ Myr and to $0.58C_s$ at $t = 4.8$ Myr, but remain subsonic throughout the evolution. The dot-dashed line is the best-fit lognormal distribution for each histogram. Both the horizontal and the vertical

axes are logarithmic (the latter being the frequency of incidence for each column-density value normalized so that the most frequent value has a frequency of 1), so the lognormal distribution has a parabolic shape. In both cases, as time progresses and density peaks develop, the width of the column-density distribution increases, but not as a result of successive compressions and rarefactions due to supersonic turbulence. The shape of the distribution remains lognormal, and a power-law tail develops at late times and at high densities. In simulation A, the power-law tails in the lognor-

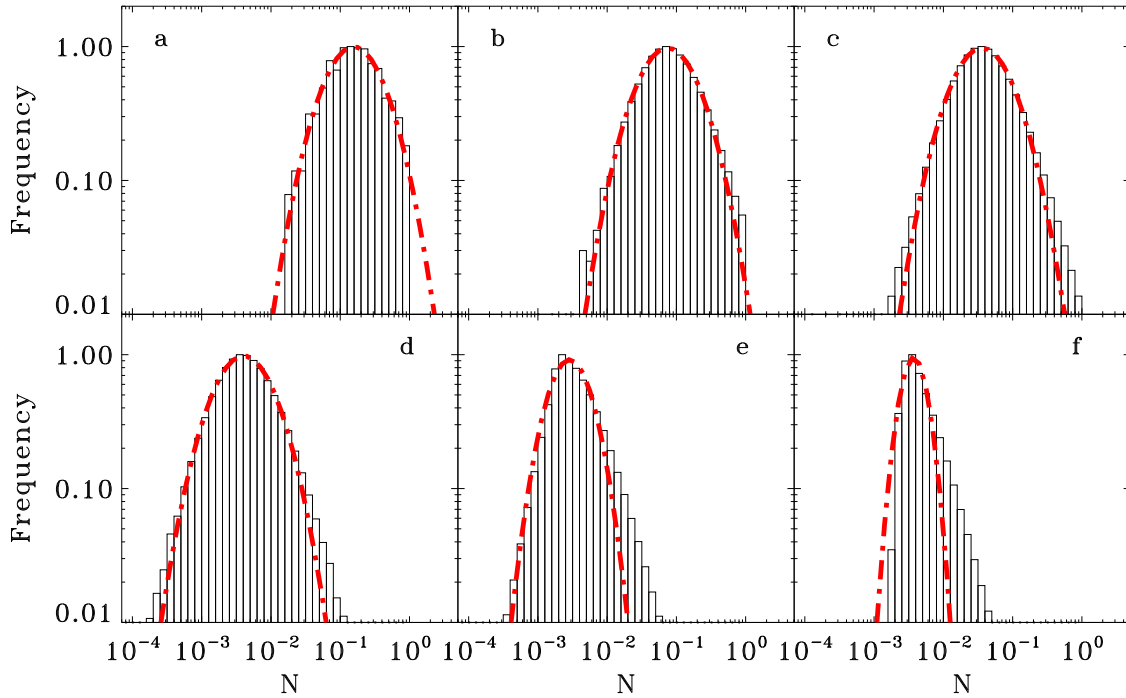


Figure 6. Column-density distribution for a cloud with a smooth density profile given by Eq. (1). *Upper row:* cloud with an extended uniform inner region and a power-law “envelope” $[(a, c) = (10, 10)]$. *Lower row:* very centrally concentrated cloud, with a very small uniform inner region and a power-law “envelope” $[(a, c) = (2, 350)]$. The middle panels in each row show the column-density distribution when the clouds are sampled on a 1024×1024 grid. The left (right) panels show the column-density distribution of the same clouds, when these are sampled with grid resolution 512×512 (2048×2048). The upper-row cloud exhibits an almost perfect lognormal column-density distribution; in the lower-row cloud the column-density distribution is also lognormal but, in addition, has a power-law tail.

mal distribution are more pronounced because of the use of sink particles that allow the simulation to continue to more advanced evolution stages, while simulation B is stopped soon after a few cores form. Power-law tails in simulation A start to appear when the fraction of mass in sink particles becomes non-negligible (3% of the mass at $t = 0.54$ Myr) and they become more pronounced as the fraction of the mass in sink particles increases (30% at $t = 0.66$ Myr, corresponding to the lower right panel of Fig. 4 with the most significant power-law tail). At low column densities, deviations from the lognormal shape are present in certain snapshots of simulation A. They appear at early times but correspond to a very small fraction of the gas in the simulated cloud. Similar deviations from the lognormal shape are also evident in observed clouds (Kainulainen et al. 2009).

The evolution is generally slower in the nonideal MHD run, since the cloud is initially magnetically subcritical, and density peaks develop only after ambipolar diffusion has had enough time to create magnetically supercritical fragments within the cloud. The simulated cloud presented here is purposely selected to be subcritical to demonstrate that, even if the magnetic forces are the dominant opposition to gravity, the formation of lognormal column-density distributions is not inhibited. The qualitative evolution of the simulation does not change with varying the initial mass-to-flux ratio; only the evolutionary timescale changes. In the case of the SPH simulation A the evolution is much faster and proceeds

on a free-fall timescale. Self-gravity dictates the evolution of the simulated cloud and is responsible for the shape of the distribution of column densities, not just its deviation from a lognormal shape at later times.

In case C, after the smooth column-density field is sampled on the 1024×1024 grid, a column density distribution is constructed using 41 bins, logarithmically spaced from 10^{-5} to 10^1 (in units of the central column density). The column-density distributions for the cloud with a substantial uniform inner region $[(a, c) = (10, 10)]$ and for the almost singular cloud $[(a, c) = (2, 350)]$ are shown in the upper and lower row middle panels (panel b and panel e) of Fig. 6, respectively. Even in this case, in which random perturbations of the density field are *completely absent*, a lognormal function fits remarkably well the distribution of the column densities. In the case of the more centrally concentrated cloud, we can also see the presence of a power-law high-density tail. In the limit of a singular isothermal-sphere profile, the column-density distribution asymptotes to a pure power-law.

We have also tested the effect of the spatial resolution of the grid, with which a column-density map is sampled, on the resulting distribution of column densities. For case C, we explicitly plot column-density distributions resulting from grids of different spatial resolutions. In each row of Fig. 6, the leftmost and rightmost panels show the same column-density distributions of the clouds as in the middle panel, but sampling occurs with grids of half and twice the spa-

tial resolution, respectively. For the cloud with a substantial uniform inner region (upper row), the grid resolution does not affect the shape of the distribution, which is, in all cases, well fitted by a lognormal. With increasing resolution, the distribution simply becomes less noisy and, as expected for an underlying density profile with a power-law tail, the most frequent column-density value decreases slightly. However, for the more centrally concentrated cloud (lower row), decreasing grid resolution leads to suppression of the power-law tails and a distribution shape better fitted by a lognormal. We have also tested the effect of smoothing down the outputs of simulations A and B to decreased spatial resolutions, and we have found that the resulting column-density distributions do not show any qualitative change - the shape of the distributions remains lognormal, with power-law tails at late times.

4 DISCUSSION AND CONCLUSIONS

The goal of this investigation has been to test whether the frequently adopted interpretation of the often observed lognormal distribution of column densities in molecular-cloud regions, i.e. that supersonic turbulence dominates the cloud dynamics, is unique or necessary. To this end, we have studied the distributions of the column density in three very different classes of model clouds: a compact and dense cloud simulated through SPH, with the evolution dominated by gravity; an isothermal, magnetically subcritical cloud with subsonic random initial velocity perturbations, with the evolution controlled by gravitationally-driven ambipolar diffusion; and a cloud with a smooth density profile, representing an isothermal, self-gravitating spherical object with a uniform inner region and a power-law profile at large radii, without any random perturbations.

We have shown that *in all cases* the column-density distributions are lognormal, with power-law tails developing at late times in simulations A and B, or, in the case of the smooth analytic profile, for very centrally concentrated configurations. *The lognormal shape of column-density distributions is not due to supersonic turbulence in any of the cases studied*, and the power-law tails are not due to intermittency or gravity taking over the dynamics. In both simulations studied here, the clouds have been self-gravitating and the evolution gravity-driven from the start, even before the development of tails. The tails develop as one or more strong density peaks appear in the simulated clouds.

Furthermore, we have tested the effect of the resolution of the grid used to sample the column density of a cloud. We have found that for an intrinsically lognormal column-density distribution, the grid resolution does not have a significant effect on the observed distribution; however, when power-law tails are present, a poor sampling resolution can suppress the tails and result in a distribution that is better fitted by a lognormal shape.

The results of this study highlight the fact that the distribution of column densities in gas clouds is a statistical characterization of the medium, and as such it does not have a one-to-one correspondence with the underlying physics that governs the dynamics of the cloud. Instead, we have found that lognormal column density distributions are a natural outcome of the evolution of a molecular cloud

regardless of whether turbulence, gravity, or ambipolar diffusion in magnetically subcritical clouds initiates or determines the evolution.

ACKNOWLEDGMENTS

We are grateful to Neal Evans for enlightening discussions. TM's work is partially supported by the National Science Foundation under grant NSF AST-07-09206 to the University of Illinois. HM is supported by the Canada Research Chair program and NSERC. This work made extensive use of the NASA Astrophysics Data System and [arXiv.org](http://arxiv.org) preprint server. AU's research was partially supported by an appointment to the NASA Postdoctoral Program at the Jet Propulsion Laboratory, administered by Oak Ridge Associated Universities through a contract with NASA. Part of this work was carried out at the Jet Propulsion Laboratory, California Institute of Technology, under a contract with the National Aeronautics and Space Administration.

©2010. All rights reserved.

REFERENCES

- Bohlin, R. C., Savage, B. D., & Drake, J. F. 1978, *ApJ*, 224, 132
 Dapp, W. B., & Basu, S. 2009, *MNRAS*, 395, 1092
 Federrath, C., Roman-Duval, J., Klessen, R., Schmidt, W., & Mac Low, M. -M. 2009, [arXiv:0905.1060](http://arxiv.org/abs/0905.1060)
 Goodman, A. A., Pineda, J. E., & Schnee, S. L. 2009, *ApJ*, 692, 91
 Hayes, J. C., Norman, M. L., Fiedler, R. A., Bordner, J. O., Li, P. S., Clark, S. E., ud-Doula, A., & Mac Low, M.-M. 2006, *ApJS*, 165, 188
 Kainulainen, J., Beuther, H., Henning, T., & Plume, R. 2009, [arXiv:0911.5648](http://arxiv.org/abs/0911.5648)
 Lombardi, M., Alves, J., & Lada, C. J. 2006, *A&A*, 454, 781
 Martel, H., Evans, N. J., II, & Shapiro, P. R. 2006, *ApJS*, 163, 122
 Monaghan, J. J. 1992, *ARA&A*, 30, 543
 Muench, A. A., Lada, C. J., Rathborne, J. M., Alves, J. F., & Lombardi, M. 2007, *ApJ*, 671, 1820
 Onishi, T., et al. 1999, *PASJ*, 51, 871
 Ostriker, E. C., Stone, J. M., & Gammie, C. F. 2001, *ApJ*, 546, 980
 Pineda, J.L., Goldsmith, P., Chapman, N., Snell, R.L., Li, D., Cambrésy, L., & Brunt, C. 2010, *submitted to ApJ*
 Urban, A., Evans, N. J., II, & Doty, S. D. 2009, *ApJ*, 698, 1341
 Urban, A., Martel, H., & Evans, N. J., II, 2010a, *ApJ*, 710, 1343
 Urban, A., Evans, N. J., II, & Martel, H., 2010b, in preparation
 Vázquez-Semadeni, E. 1994, *ApJ*, 423, 681
 Vázquez-Semadeni, E., & García, N. 2001, *ApJ*, 557, 727
 Wong, T., et al. 2008, *MNRAS*, 386, 1069